Electron-paramagnetic-resonance study of the Pd^{3+} Jahn-Teller ion in CaO

A. Raizman, J. Barak, and J. T. Suss
Solid State Physics Department, Soreq Nuclear Research Center, Yavne 70600, Israel
(Received 29 August 1984)

The electron-paramagnetic-resonance spectrum of Pd^{3+} was studied in a single crystal of CaO at X-band frequency. The spectrum exhibits an intermediate quadrupole interaction and a static Jahn-Teller effect. The Jahn-Teller distortions produce the electric field gradient required for the quadrupole interaction. At high temperatures the spectrum is isotropic, and at low temperatures it consists of a superposition of three tetragonal spectra. It could be concluded that the first excited vibronic level is a singlet A_1 and $\overline{\delta}/3\Gamma \approx 5$. The anomalous effects in the hyperfine structure, caused by the relatively large quadrupole interaction ($Q/A_\perp \approx 0.59$), were interpreted by an exact diagonalization of the spin Hamiltonian.

I. INTRODUCTION

Ions possessing orbitally degenerate electronic ground states are known to be subject to the Jahn-Teller (JT) effect. We report here an electron-paramagnetic-resonance (EPR) study of the Pd^{3+} JT ion in single crystals of CaO. The electronic configuration of Pd^{3+} is $4d^7$, and like other ions of the $4d$ and $5d$ groups it belongs to the "strong-ligand-field" category (low-spin case). In octahedral symmetry the low-spin ground state of Pd^{3+} is the orbital doublet ^2E_g ($t_{2g}^6 e_g^1$), subject to the JT effect.[1] Palladium has an odd isotope, ^{105}Pd with natural abundance 22.23%, nuclear spin $I=\frac{5}{2}$, and quadrupole moment $Q_0=+0.8$ b.[2] Nuclear quadrupole interaction (QI) is usually much smaller than hyperfine interaction (HI), and thus can be treated by the usual perturbation-theory formulas.[3] In the case of Pd^{3+} in CaO, the QI is quite strong ($Q/A_\perp \approx 0.59$, as is shown below), and an exact diagonalization of the spin Hamiltonian is necessary for the correct interpretation of the spectrum. Several cases of strong QI for ions having $I=\frac{3}{2}$ have been treated extensively in the past.[4,5] To the best of our knowledge the case of Pd^{3+} is the first clear experimental evidence of strong QI for an ion with $I=\frac{5}{2}$. In addition to the interpretation of the specific case of Pd^{3+} in CaO, we also present here calculated results for the behavior of an EPR spectrum with $I=\frac{5}{2}$ at $g_\perp$ as a function of $Q/A_\perp$. The EPR spectrum of Pd^{3+} (without any treatment of the QI) was reported previously in single crystals of K_2PdCl_4, $(NH_4)_2PdCl_4$,[6] and MgO,[7,8] and in powders of CaO (Ref. 9) and Al_2O_3 (Ref. 10).

II. EXPERIMENTAL DETAILS

Single crystals of CaO doped with Pd were grown for us by W.&C. Spicer Ltd., by melting 10-kg $CaCO_3$ with 0.2-mol% $PdCl_2$ powder in an electric arc furnace. The growth yielded over 1 kg of melt from which the single crystals for our experiments could be easily harvested. The arc-grown crystals were milky and slightly yellowish. A Varian X-band EPR spectrometer was used at several temperatures in the range between 1.65 and 230 K. The spectrum of Pd^{3+} ions was observed in the as-grown crystals. The fitting of the spin-Hamiltonian parameters were carried out with an IBM 370/160 computer using the FORTRAN IV version of the MAGNSPEC program.[11]

III. RESULTS

The spin Hamiltonian for Pd^{3+} is composed of the electronic Zeeman term, the HI, the nuclear QI, and the nuclear Zeeman term

$$\mathcal{H}=\mu_B \mathbf{S}\cdot\tilde{g}\cdot\mathbf{H}+\mathbf{S}\cdot\tilde{A}\cdot\mathbf{I}+\mathbf{I}\cdot\tilde{Q}\cdot\mathbf{I}-g_N\mu_N\mathbf{I}\cdot\mathbf{H} \quad (1)$$

where μ_B is the Bohr magneton, $\mathbf{S}$ the electronic spin, $\tilde{g}$ the g tensor, $\mathbf{H}$ the external magnetic field, $\tilde{A}$ the hyperfine tensor, $\mathbf{I}$ the nuclear spin, $\mathbf{Q}$ the quadrupole tensor, and g_N and μ_N the nuclear g factor and magneton, respectively.

In the temperature range between 1.65 and 4.2 K the experimental spectrum consists of a superposition of three tetragonal spectra with symmetrical line shapes. These spectra can be fitted to the axial spin Hamiltonian derived from Eq. (1), for $\mathbf{H}$ in the x-z plane,

$$\mathcal{H}=g_{||}\mu_B S_z H_z+g_\perp\mu_B S_x H_x+A_{||}I_z S_z+A_\perp I_x S_x +Q[I_z^2-\tfrac{1}{3}I(I+1)]-g_N\mu_N(I_z H_z+I_x H_x) \quad (2)$$

where $H_x=H\sin\theta$, $H_z=H\cos\theta$, and $g_N=-0.256$.[2]

For the stable even isotopes of Pd ($S=\frac{1}{2}$, $I=0$), only one transition is expected (the strong central line of the spectrum) for each tetragonal site. This set is described by the electronic Zeeman interaction given by the first two terms of the Hamiltonian in Eq. (2). The angular dependence of this central line in a (100)-type plane at 4.2 K is shown in Fig. 1. It agrees well with the octahedral symmetry of the CaO crystal and with the axial g tensors whose directions are randomly distributed among the three $\langle 100\rangle$-type axes. The g values at 4.2 K were measured to be $g_{||}=2.0109(5)$, $g_\perp=2.2212(5)$, and $g_{[111]}=2.1540(5)$. The low-temperature spectra at 4.2 K, due to both even and odd isotopes of Pd^{3+} at $g_\perp$ and $g_{[110]}$ are shown in Figs. 2 and 3, respectively. At high tempera-

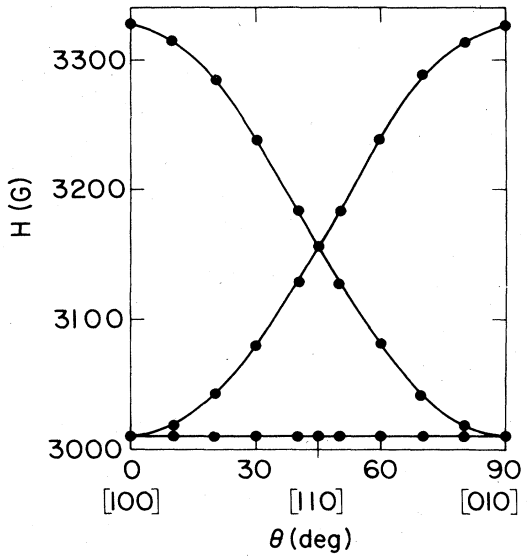

FIG. 1. Angular dependence (only the central line of the spectrum, due to the stable even isotopes of Pd) of the Pd^{3+} ion in CaO, in the (100) plane, at 4.2 K and 9.4 GHz. The points represent the measured values for the resonance line due to Pd nuclei with $I=0$.

tures (>77 K) the spectrum is isotropic with $g=2.153(1)$ at 93 K (see spectrum in Fig. 4), which agrees with the g factor measured at low temperature in the [111] direction (see Table I).

We have used the MAGNSPEC computer program[11] to simulate, from Eq. (2), the EPR transitions, and to calculate, by "trial and error," the parameters $A_{||}$, $A_{\perp}$, and Q for our spectra. It is preferable to start with the spectrum for $\theta=90°$ since the Hamiltonian has a simpler form and less transitions are expected. In order to have a good

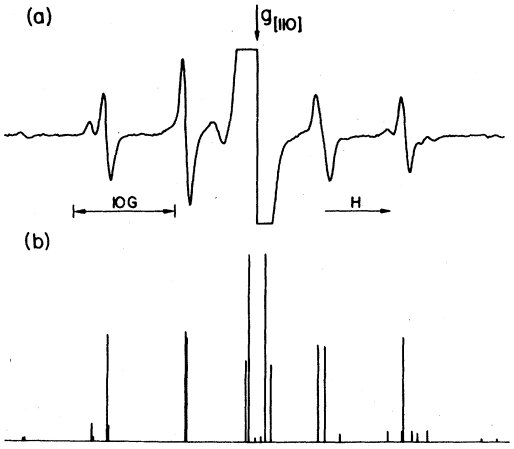

FIG. 3. Same as Fig. 2, but at $g_{[110]}$.

"first guess" of the magnitude of $Q/A_{\perp}$, we have calculated the dependence of the transitions on $Q/A_{\perp}$ for $\mathscr{H}$ in Eq. (2) for $S=\frac{1}{2}, I=\frac{5}{2}$. For simplicity, the nuclear Zeeman term was excluded in these calculations. The calculated transitions are plotted in Fig. 5.

For $\theta=90°$ the energy matrix, with dimensions 6×6, for either $M=\frac{1}{2}$ or $-\frac{1}{2}$, is divided into two 3×3 matrices, giving rise to 18 allowed transitions of $\Delta M=1$ and $\Delta m=0,2,4$. As long as the nuclear Zeeman term is omitted, the spectra have a mirror symmetry around H_0, which is the resonance field of the spinless ($I=0$) nuclei. For $Q/A_{\perp}\rightarrow0$, the off-diagonal terms of the matrix become small and we expect only six equidistant lines with $\Delta m=0$, separated by $A_{\perp}$.[3] In a recent paper we discussed the other extreme case, namely that of $|Q/A_{\perp}|\gg1$.[5] The nuclear spins are quantized in the direction of the

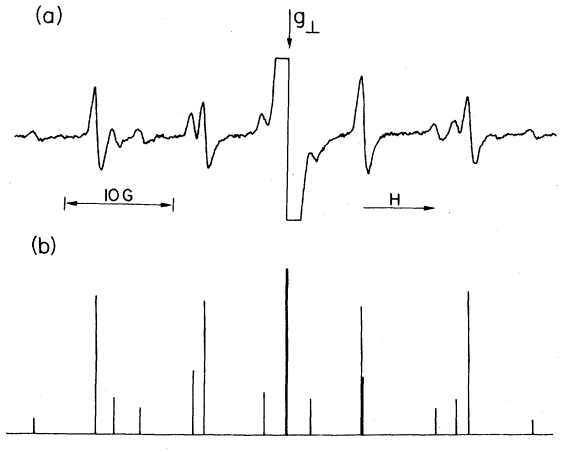

FIG. 2. EPR spectra of Pd^{3+} in CaO at $g_{\perp}$, 4.2 K and 9.4 GHz. (a) The recorded spectrum. (b) The calculated spectrum. The spectrum should be flanked on each side by one weak line (not shown), which could sometimes be observed under favorable experimental conditions.

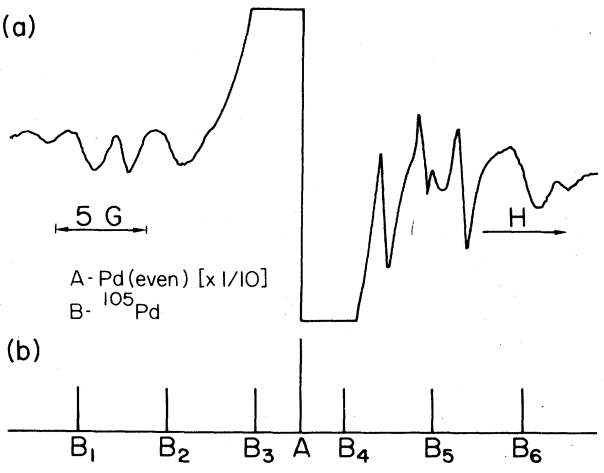

FIG. 4. High-temperature isotropic spectrum of Pd^{3+} in CaO at 93 K, 9.4 GHz, and with **H** along a [111]-type direction. (a) The recorded spectrum. (b) The calculated spectrum. Some of the hyperfine lines in the recorded spectrum are obscured by resonance lines due to other impurities, mainly Mn^{2+}.

TABLE I. Resonance and nuclear parameters for Pd^{3+} ($S=\frac{1}{2}, I=\frac{5}{2}$) in CaO.

		T (K)
g	$g_{\|\|}=2.0109(5)$	4.2
	$g_{\perp}=2.2212(5)$	4.2
	$g_{[111]}=2.1540(5)$	4.2
	$(g_{\|\|}+2g_{\perp})/3=2.1511$	
	$g_{[111]}=2.153(1)$	93
	$g_N=-0.256$[a]	
A (10^{-4} cm^{-1})	$A_{\|\|}=0.5(1)$	4.2
	$A_{\perp}=6.8(1)$	4.2
	$(A_{\|\|}+2A_{\perp})/3=4.7$	
	$A_{[111]}=4.9(5)$	93
Q_0 (b)	$Q_0=0.8$[a]	

[a]Reference 2.

symmetry of the QI, with quantum numbers $\bar{m}$, rather than in the direction of the external magnetic field. For $|Q/A_{\perp}|\to\infty$ only the six "$\Delta\bar{m}=0$" transitions are allowed. These lines are marked on the right-hand side of Fig. 5. There is a strong central line for the four transitions between levels with $|\bar{m}|\neq\frac{1}{2}$, with two satellites at a distance $3A_{\perp}/2$ away on both sides. The $|-\frac{1}{2}\rangle \leftrightarrow |-\frac{1}{2}\rangle$ transition is observed at the high-field side for $A_{\perp}>0$.

The spectrum of Fig. 2 does not resemble any of the spectra for the two extremes of $|Q/A_{\perp}|$. The spectrum

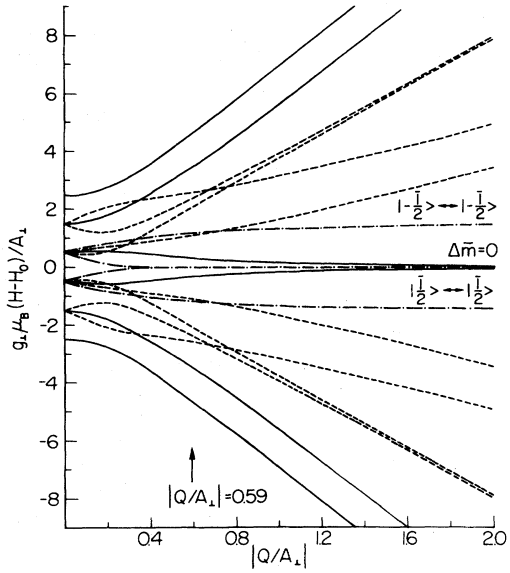

FIG. 5. Dependence of the EPR spectrum of an ion with $S=\frac{1}{2}$ and $I=\frac{5}{2}$ on $|Q/A_{\perp}|$, at $\theta=90°$. The solid lines represent the allowed transitions at $Q/A_{\perp}=0$ ($\Delta m=0$). The dashed lines, $\Delta m=2$ (— — —) and $\Delta m=4$ (— · — · —), are forbidden at $Q/A_{\perp}=0$, but have finite probability for $Q/A_{\perp}\neq 0$. $|Q/A_{\perp}|=0.59$ gives the best fit for ^{105}Pd for the case of Pd^{3+} in CaO.

is fitted to an intermediate value of $|Q/A_{\perp}|$. The best-fit value, $|Q/A_{\perp}|\approx 0.59$, is marked by an arrow in Fig. 5.

The experimental spectra (see Figs. 2 and 3) are asymmetrical with respect to the central line. This is due to the nuclear Zeeman term. In our case it is not negligible compared to Q and $A_{\perp}$. It enabled us to determine the relative signs of Q, $A_{\|}$, and $A_{\perp}$. The asymmetry is reversed when the sign of either both $A_{\|}$ and $A_{\perp}$, or Q (or the sign of g_N), is reversed. For $g_N<0$,[2] the experimental results are compatible with $A_{\perp}/A_{\|}>0$ and $Q/A_{\perp}<0$. As discussed below, we believe that Q is negative. The parameters which give the best fit at all angles are $A_{\perp}=6.8(1)\times 10^{-4}$ cm^{-1}, $A_{\|}=0.5(1)\times 10^{-4}$ cm^{-1}, and $Q=-4.0(1)\times 10^{-4}$ cm^{-1}. Table I summarizes the parameters of the spin Hamiltonian. The stick diagrams of Figs. 2 and 3 were drawn using these parameters and they show very good agreement with the experimental results. For $\theta=90°$ we expect 18 resonance lines with different intensities, while for $\theta\neq 90°$ there might be up to 36 lines due to the off-diagonal terms in the Hamiltonian. The lines disappear or join the main line for $\theta\to 0$. We could observe all the calculated lines which were sufficiently strong to be detected and which were not masked by the main central line (due to $I=0$ nuclei). This also includes very weak lines on each side of the spectrum outside the range of Figs. 2 and 3. The angular variation of the lines could be followed in the range $15°<\theta<90°$. The hyperfine constant, $A_{[111]}=4.9(5)\times 10^{-4}$ cm^{-1}, extracted from the high-temperature spectrum at 93 K in the [111] direction (see Fig. 4 and Table I), agrees with $\bar{A}=(A_{\|}+2A_{\perp})/3=4.7\times 10^{-4}$ cm^{-1}.

The quadrupole constant Q is given by the product of the quadrupole moment Q_0 and the electric field gradient at the nuclear site, in the direction of the axial symmetry, $V_{zz}\equiv eq$,

$$Q=\frac{3e^2qQ_0}{4I(2I-1)}\ . \tag{3}$$

There are two contributions to q: $q_{\rm val}$, due to the $4d$ valence electrons of the Pd^{3+} ion, and $q_{\rm latt}$, due to the charges of the ligand ions. Both are shielded by the core electrons as given by the corresponding Sternheimer factors. Thus,[3]

$$q=(1-R)q_{\rm val}+(1-\gamma_{\infty})q_{\rm latt}\ . \tag{4}$$

The axial symmetry of a d electron gives rise to

$$q_{\rm val}=-\langle r^{-3}\rangle N_{\sigma}^2\langle l||\alpha||l\rangle[3l_z^2-l(l+1)]\ , \tag{5}$$

where $\langle r^{-3}\rangle$ is the mean inverse third power of the electron distance from the nucleus, averaged over the electron wave functions. N_{σ}^2 is the covalency coefficient, $N_{\sigma}^2\leq 1$. For Pd^{3+} (configuration $4d^7$) in a strong octahedral crystal field, six of the d electrons are in the closed t_{2g} shell. The remaining electron is in the $|\theta\rangle$ state, a $3z^2-r^2$ orbital, as deduced from the g factors ($g_{\|}<g_{\perp}$). This state has $l=2$, $l_z=0$, and $\langle l||\alpha||l\rangle=-\frac{2}{21}$. Thus $q_{\rm val}$ will be negative and given by

$$q_{\rm val}=-\tfrac{4}{7}N_{\sigma}^2\langle r^{-3}\rangle\ . \tag{6}$$

For calculating q_{latt}, let the Pd^{3+} impurity substitute for a Ca^{2+} ion in site (0,0,0), which has six O^{2-} first neighbors in an octahedron a distance $d=a_0/2$ from (0,0,0), where $a_0=4.81$ Å is the lattice constant. For the $|\theta\rangle$ state of Pd^{3+} this octahedraon is elongated ($\delta>0$) and the oxygen ions occupy the sites $(d-\delta,0,0)$, $(-d+\delta,0,0)$, $(0,d-\delta,0)$, $(0,-d+\delta,0)$, $(0,0,d+2\delta)$, and $(0,0,-d-2\delta)$, where 2δ is the amount of the elongation of the Pd^{3+}–O^{2-} bond along the z direction. This gives rise to an electric field gradient which, for two negative charge units at each of the above points and $\delta \ll d$, is given by

$$q_{\text{latt}}=72\delta/d \ . \tag{7}$$

Since $\delta>0$, q_{latt} and q_{val} will have opposite signs. $1-R$ and $1-\gamma_\infty$ are both positive. Thus it follows from Eq. (4) that $|q|$ will be smaller than either of the terms in this equation. The sign of q will be negative if

$$|(1-R)q_{\text{val}}| > |(1-\gamma_\infty)q_{\text{latt}}| \ .$$

In calculating q we use the following values: $\langle r^{-3}\rangle=5.73\times10^{25}$ cm^{-3},[12] $1-R\approx0.7$, and $N_\sigma^2\approx0.8$. Equations (3), (4), and (6) will give a quadrupole constant due to the valence electrons, $Q_{\text{val}}\approx-12.75\times10^{-4}$ cm^{-1}. For the lattice part, , Q_{latt}, we take $2\delta\approx0.1$ Å, as is later obtained from the calculated vibronic parameters, and $1-\gamma_\infty\approx50$. With $d=a_0/2=2.405$ Å, this gives $Q_{\text{latt}}\approx3.75\times10^{-4}$ cm^{-1}. The sum of the two contributions is $Q=Q_{\text{val}}+Q_{\text{latt}}\approx-9\times10^{-4}$ cm^{-1}. This value is about twice the experimental value (-4.0×10^{-4} cm^{-1}). Owing to the smaller ionic radius and larger positive charge of Pd^{3+}, compared with those of Ca^{2+}, the Pd^{3+}–O^{2-} bonds are expected to be smaller than $a_0/2$, and the Q_{latt} larger than calculated above. In view of this and the uncertainties in the values of R, γ_∞, N_σ^2, $\langle r^{-3}\rangle$, and δ, we believe that the analysis given here explains the origin of the quadrupole interaction in our case.

It is interesting to compare our case to other JT ions in a cubic site. Such is the case of Ir^{2+} in CaO and MgO,[4] where, by arguments similar to those given above, it can be shown that there $|Q_{\text{val}}| \gg |Q_{\text{latt}}|$ as well. The case of Cu^{2+} in CaO is different. There, no QI could be detected, either for the $|\theta\rangle$ state of for the $|\epsilon\rangle$ state (x^2-y^2 orbital).[13] For the copper nuclei with $I=\frac{3}{2}$, $Q_0=-0.2$ b, $\langle r^{-3}\rangle\approx5.57\times10^{25}$ cm^{-3}, $1-R\approx0.7$, $1-\gamma_\infty\approx20$, and $N_\sigma^2\approx0.8$, one obtains, for the d^9 $|\theta\rangle$ state, $Q_{\text{val}}\approx-10^{-3}$ cm^{-1}, which should be observable. It might be thus concluded that this is the case where $Q_{\text{latt}}=-Q_{\text{val}}$. The $4d$ ions are known to form more covalent bonds than the $3d$ ions, leading to a larger overlap of the Pd^{3+} wave function with the neighboring O^{2-} ions. Thus the distortion of the ligand octahedron will be smaller and the negative Q_{val} will be dominant. All these considerations make us believe that $Q<0$ for Pd^{3+} in CaO.

IV. DISCUSSION

Inspection of the g factors given in Table I shows that $g_{\|}<g_\perp$. This indicates, for the $^2E_g(t_{2g}^6e_g^1)$ configuration, an elongated octahedron with a ground state E_θ, when the distortion of the octahedron is along the z direction. For this case the first-excited singlet is A_1, and for a strong JT coupling ($q=\frac{1}{2}$), $g_{\|}=g_1-g_2$ and $g_\perp=g_1+\frac{1}{2}g_2$.[14] The positive g shift ($g_{\|}-g_e$) for an E_θ state in our case can be explained by the second-order contribution due to terms of the form $(\xi/\Delta_i)^2$ to the g factor. Here, g_e is the free-electron g factor (2.0023), ξ is the spin-orbit–coupling coefficient, and the Δ_i are the separations between the ground state E due to the $t_{2g}^6e_g^1$, and the excited energy levels due to the $t_{2g}^5e_g^2$, crystal-field configurations. This contribution is mainly due to the $^4T_1$ energy level and becomes appreciable near the crossover (at $Dq/B=2.15$) of the ^2E and $^4T_1$ levels in the Tanabe-Sugano[15] diagram for a d^7 configuration. A positive g shift was also obtained for the isoelectronic Rh^{2+} ion ($4d^7$ configuration) in MgO (Ref. 7) and CaO (Ref. 16). Since Pd^{3+} has a higher charge than Rh^{2+}, plus it is expected that the Pd^{3+} ion will be exposed to a stronger crystalline electric field than Rh^{2+}, causing larger splitting of the electronic energy levels and thus also a larger value of Dq/B. It is therefore reasonable that the positive g shift observed for Pd^{3+} in CaO is smaller than that for Rh^{2+}. On the other hand, a negative g shift was observed in $5d^7$ ions: Pt^{3+} in MgO (Ref. 17) and Ir^{2+} in MgO and CaO (Ref. 4). These observations are in agreement with the well-known increase in the crystal-field strength upon going from a $4d^n$ ion to a $5d^n$ one.

An estimation of the core-polarization contribution to the hyperfine splitting constant can be obtained from the high-temperature hyperfine splitting constant (see Table I) using the expression[3]

$$A=P(g_L-\kappa)$$

and neglecting covalent effects. Here,

$$P=2\gamma_N\mu_B\mu_N\langle r^{-3}\rangle \ ,$$

γ_N is the nuclear magnetogyric ratio, and κ is the core-polarization factor. $g_L\equiv g-g_e$ is the difference between the measured and the free-electron g factor. The above equation yields $\kappa=0.23$, and, consequently, for χ, a quantity characteristic of the unpaired spin at the nucleus and related to κ by [3] $\chi=-\frac{3}{2}\kappa\langle r^{-3}\rangle$, we obtained $\chi=-2.9$ a.u. Freeman *et al.*[18] calculated χ for $4d$ ions and obtained values between -8 and -9 a.u. Our deviation from the calculated value of χ may be due to covalent effects and partial admixing of a $5s$ wave function, which gives rise to a positive contribution to the isotropic hyperfine interaction.

We shall now discuss the parameters of the vibronic Hamiltonian, summarized in Table II. As mentioned above, the first-excited singlet is A_1, and thus V and β, the linear and nonlinear JT coupling coefficients, respectively, are positive. The ratio $\bar{\delta}/3\Gamma$ (where $\bar{\delta}$ is the mean random strain splitting of the vibronic doublet E, and 3Γ is the tunneling splitting between the doublet E and the first-excited singlet A_1) estimated from the line shape and the angular dependence[19,20] of the low-temperature spectrum is approximately 5. The angular dependence corresponds to three tetragonally symmetric spectra with a symmetric line shape. However, at $g_{\|}$ the dominant central line (due to the even isotopes) undergoes a broadening.

TABLE II. Vibronic parameters for Pd^{3+} in CaO.

$\bar{\delta}/3\Gamma$	$\simeq 5$
V_s, strain coupling coefficient (cm^{-1})	1.79×10^4
$\bar{\delta}$, mean random strain splitting (cm^{-1})	3.6
3Γ, tunneling splitting (cm^{-1})	0.7
V, linear JT coupling coefficient ($erg\,cm^{-1}$)	1.28×10^{-4}
$\hbar\omega$, energy of the E_g mode vibration (cm^{-1})	300
E_{JT}, Jahn-Teller energy (cm^{-1})	480
ρ_0, equilibrium value of the radial coordinate ρ (Å)	0.17
$E_{JT}/\hbar\omega$	1.6
α, rotational kinetic energy (cm^{-1})	47
2β, height of barrier separating adjacent wells (cm^{-1}). (β is the nonlinear JT coupling coefficient.)	2100
Δ, splitting between A_1 and A_2 (cm^{-1})	840
$\Delta\omega_L=2\pi\nu(g_\perp-g_{\|})/g_{[111]}$ (sec^{-1})	5.7×10^9
T_t, transition temperature at which the transition from low- to high-temperature spectrum occurs (K)	$4.2<T_t<77$

The strain coupling coefficient V was calculated according to Ham,[21] and, using $\langle r^2\rangle=1.94$ a.u. and $\langle r^4\rangle=6.59$ a.u.,[12] gives $V_s=1.79\times10^4$ cm^{-1}. A value of $V_s=2.75\times10^4$ cm^{-1} was calculated for Ir^{2+} in CaO.[4] $V_s=2.6\times10^4$ cm^{-1} was determined for Cu^{2+} in CaO by using results of an experiment where external stress was applied.[22]

The mean random strain splitting is defined[14] as $\bar{\delta}=2qV_s\,(e_\theta^2+e_\epsilon^2)^{1/2}$, where e_θ and e_ϵ are the θ and ϵ components of the strain tensor e, respectively. Assuming a value of $q=\frac{1}{2}$ for the Ham reduction factor and taking a typical residual strain[23] $e\approx2\times10^{-4}$, we obtained $\bar{\delta}=3.6$ cm^{-1}, and, consequently, the tunneling splitting, $3\Gamma=0.7$ cm^{-1}.

Following Ham's[14] analysis, one can calculate the linear JT coupling coefficient V and the JT energy E_{JT}, $V=(\sqrt{3}/2R)V_s$ and $E_{JT}=V^2/2\mu\omega^2$. μ and ω are the effective mass and the angular frequency of the vibrational modes, respectively. For μ we used the mass of a single oxygen atom and ω was taken as $\omega=300$ cm^{-1}.[1] We obtained, for the JT stabilization energy, $E_{JT}=480$ cm^{-1}. E_{JT} corresponds to the equilibrium value $\rho=\rho_0=|V|/\mu\omega^2$. ρ is the radial coordinate of the vibrational modes. From this relationship we obtain $\rho=0.17$ Å. From this the difference between the elongated Pd^{3+}–O^{2-} bond lengths as compared with the undistorted octahedron can be calculated as $\rho_0/\sqrt{3}\approx0.1$ Å. The value of $E_{JT}/\hbar\omega$ is 1.6. For $E_{JT}/\hbar\omega\gtrsim1$ the rotational kinetic energy is given quite accurately[14] as $\alpha=\hbar\omega(4E_{JT}/\hbar\omega)^{-1}$, which yields $\alpha=47$ cm^{-1}. The nonlinear JT coupling coefficient β and the energy splitting Δ between the first-excited vibronic singlet A_1 and the next-lowest singlet A_2 can be found from graphs given by Williams *et al.*[24] We obtained $\beta=1050$ cm^{-1} and $\Delta=840$ cm^{-1}.

As pointed out above, the temperature T_t at which the transition from the low-temperature anisotropic spectrum to the high-temperature isotropic spectrum of Pd^{3+} in CaO occurs is between 4.2 and 77 K. The high-temperature spectrum seems to be mainly due to the motional-averaging process, since at 77 K the population of the excited singlet A_2 is negligible. Further support for this is given by the behavior of the linewidth of the isotropic (high-temperature) spectrum as a function of temperature and the external magnetic field. It exhibits behavior typical of a motionally averaged JT ion,[25] in the form of a monotonic increase of the linewidth with **H** along a [111] direction, and a minimum in the linewidth along a [100] direction. This effect was explained qualitatively by a combination of two relaxation mechanisms. One mechanism is due to motional averaging ($\Delta\omega_L\tau$) and causes the linewidth to decrease with increasing temperature. Here, $\Delta\omega_L$ is the difference between the Larmor frequencies of the corresponding resonance lines for the different distorted configurations and τ^{-1} is the rate of the motional averaging. The contribution of the motional averaging is also dependent on the direction of the external magnetic field **H**, i.e., it is zero with **H** along the [111] direction and maximum with **H** along the [100] direction. The other mechanism is due to spin-lattice–relaxation effects and causes an increase in linewidth with increasing temperature. At high temperatures, where the mechanism of spin-lattice–relaxation effects is dominant, an isotropic linewidth is obtained. The superposition of these two relaxation mechanisms causes a minimum in the linewidth-versus-temperature relationship, except in the [111] direction, where the contribution to the motional averaging vanishes.[4]

V. SUMMARY

The EPR spectrum of Pd^{3+} in CaO exhibits a clear case of a static JT effect and an intermediate QI with $Q/A_\perp\approx0.59$. The EPR spectra could be precisely characterized by a single spin Hamiltonian for $S=\frac{1}{2}$ with nuclear terms for ^{105}Pd with $I=\frac{5}{2}$. The Hamiltonian is discussed for various values of $Q/A_\perp$ and the parameters appropriate for our case are summarized in Table I. The electric field gradient required for the QI is caused by the JT distortions. The main contribution is due to the $|\theta\rangle$

orbital of Pd^{3+} which gives rise to $Q<0$. The asymmetry of the spectra, caused by the nuclear Zeeman interactions with $g_N<0$, enabled us to determine that the signs of $A_{||}$ and $A_{\perp}$ are positive. From the behavior of the spectra ($g_{\perp}>g_{||}$), it could be concluded that the first-excited vibronic level is a singlet A_1, and that V and β, the linear and nonlinear JT coupling coefficients, respectively, are positive. The calculated vibronic parameters are summarized in Table II.

ACKNOWLEDGMENT

We are grateful to R. Englman for helpful discussions.

[1]R. Englman, *Jahn-Teller Effect in Molecules and Crystals* (Wiley, New York, 1972).
[2]G. C. Carter, L. H. Bennett, and D. J. Kahan, *Metallic Shifts in NMR* (Pergamon, Oxford, 1977), Pt. I, p. 289.
[3]A. Abragam and B. Bleaney, *Electron Paramagnetic Resonance of Transition Ions* (Oxford University Press, Oxford, 1970).
[4]A. Raizman J. T. Suss, and W. Low, Phys. Rev. B **15**, 5184 (1977), and references therein.
[5]J. Barak, A. Raizman, and J. T. Suss, J. Magn. Res. **53**, 23 (1983), and references therein.
[6]T. Krigas and M. T. Rogers, J. Chem. Phys. **54**, 4769 (1971).
[7]J. T. Suss, A. Raizman, S. Shapiro, and W. Low, J. Magn. Res. **6**, 438 (1972).
[8]B. Barnet, A. Raizman, and J. T. Suss, Bull. Israel Phys. Soc. **22**, 26 (1976).
[9]P. Wysling, K. A. Müller, and W. Höchli, Helv. Phys. Acta **38**, 358 (1965).
[10]R. Lacroix, U. Höchli, and K. A. Müller, Helv. Phys. Acta **37**, 627 (1964).
[11]J. M. Mackey, M. Kopp, E. C. Tynan, and Teh Fu Yen, in *ESR of Metal Complexes,* edited by Teh Fu Yen (Plenum, New York, 1969), p. 33.
[12]A. J. Freeman and R. E. Watson, in *Magnetism,* edited by G. T. Rado and H. Suhl (Academic, New York, 1965), Vol. 2A, Chap. 4, pp. 167–305.
[13]A. Raizman, J. Barak, R. Englman, and J. T. Suss, Phys. Rev. B **24**, 6262 (1981); J. Barak, A. Raizman, and J. T. Suss, Bull. Magn. Res. **5**, 215 (1983).
[14]F. S. Ham, in *Electron Paramagnetic Resonance,* edited by S. Geschwind (Plenum, New York, 1972), p. 1.
[15]Y. Tanabe and S. Sugano, J. Phys. Soc. Jpn. **9**, 753 (1954).
[16]A. Raizman and J. T. Suss, in *Magnetic Resonance and Related Phenomena,* proceedings of the 18th AMPERE Congress, edited by P. S. Allen, E. R. Andrew, and C. A. Bates (North-Holland, Amsterdam, 1975), Vol. I, p. 121.
[17]A. Raizman, A. Schoenberg, and J. T. Suss, Phys. Rev. B **20**, 1863 (1979).
[18]A. Freeman, J. V. Mallow, and P. S. Bagus, J. Appl. Phys. **41**, 1321 (1970).
[19]R. W. Reynolds and L. A. Boatner, Phys. Rev. B **12**, 4735 (1975).
[20]L. A. Boatner, R. W. Reynolds, Y. Chen, and M. M. Abraham, Phys. Rev. B **16**, 86 (1977).
[21]F. S. Ham, Phys. Rev. B **11**, 3854 (1971).
[22]S. Guha and L. L. Chase, Phys. Rev. B **12**, 1658 (1975); see also S. Guha and L. L. Chase, Phys. Rev. Lett. **32**, 869 (1974).
[23]A. M. Stoneham, Proc. Phys. Soc. London **89**, 909 (1966).
[24]F. I. B. Williams, D. C. Krupka, and D. P. Breen, Phys. Rev. **179**, 225 (1969).
[25]D. P. Breen, D. C. Krupka, and F. I. B. Williams, Phys. Rev. **179**, 241 (1969).